\



Disorder in parity-time symmetric quantum walks

Peng Xue(薛鹏)

Citation: Chin. Phys. B, 2022, 31 (**1**): 010311. DOI: 10.1088/1674-1056/ac3741
Journal homepage: http://cpb.iphy.ac.cn; http://iopscience.iop.org/cpb

What follows is a list of articles you may be interested in

Two-body exceptional points in open dissipative systems

Peize Ding(丁霈泽) and Wei Yi(易为)
Chin. Phys. B, 2022, 31 (**1**): 010309. DOI: 10.1088/1674-1056/ac3396

Efficient and stable wireless power transfer based on the non-Hermitian physics

Chao Zeng(曾超), Zhiwei Guo(郭志伟), Kejia Zhu(祝可嘉), Caifu Fan(范才富), Guo Li(李果), Jun Jiang(江俊), Yunhui Li(李云辉), Haitao Jiang(江海涛), Yaping Yang(羊亚平), Yong Sun(孙勇), and Hong Chen(陈鸿)
Chin. Phys. B, 2022, 31 (**1**): 010307. DOI: 10.1088/1674-1056/ac3815

High winding number of topological phase in non-unitary periodic quantum walk

Yali Jia(贾雅利) and Zhi-Jian Li(李志坚)
Chin. Phys. B, 2021, 30 (**10**): 100301. DOI: 10.1088/1674-1056/abf554

Anti-parity-time symmetric phase transition in diffusive systems

Pei-Chao Cao(曹培超) and Xue-Feng Zhu(祝雪丰)
Chin. Phys. B, 2021, 30 (**3**): 030505. DOI: 10.1088/1674-1056/abd694

Exact scattering states in one-dimensional Hermitian and non-Hermitian potentials

Ruo-Lin Chai(柴若霖), Qiong-Tao Xie(谢琼涛), Xiao-Liang Liu(刘小良)
Chin. Phys. B, 2020, 29 (**9**): 090301. DOI: 10.1088/1674-1056/ab928f

---

SPECIAL TOPIC — Non-Hermitian physics

Disorder in parity–time symmetric quantum walks

Peng Xue(薛鹏)[†]

Beijing Computational Science Research Center, Beijing 100084, *China*

(Received 2 October 2021; revised manuscript received 4 November 2021; accepted manuscript online 6 November 2021)

We experimentally investigate the impact of static disorder and dynamic disorder on the non-unitary dynamics of parity–time (PT)-symmetric quantum walks. Via temporally alternating photon losses in an interferometric network, we realize the passive PT-symmetric quantum dynamics for single photons. Controllable coin operations allow us to simulate different environmental influences, which result in three different behaviors of quantum walkers: a standard ballistic spread, a diffusive behavior, and a localization, respectively, in a PT-symmetric quantum walk architecture.

Keywords: parity–time symmetry, quantum walks, disorder

PACS: 03.67.Lx, 03.67.Hk, 05.40.Fb, 05.45.Mt **DOI:** 10.1088/1674-1056/ac3741

1. Introduction

One of the fundamental features of quantum mechanics is associated with the Hermiticity of Hamiltonian operators, which implies both real eigenenegies and conserved probabilities. Recently, more and more attention is attracted by a wide class of non-Hermitian Hamiltonians with party–time (PT) symmetry,[1] which still show entirely real spectra. PT-symmetric dynamics have been implemented in various physical systems,[2–14] where PT-related notions and behaviors can be observed and experimentally investigated.[15–22] However, the effect of disorder in a non-Hermitian system is still less investigated.

It is well known that static disorder leads to an absence of diffusion and the wavefunction of the particle becomes localized, which was first predicted by Anderson in 1958.[23] The so-called Anderson localization has been investigated in various physical systems, for example, photons in semiconductor powders,[24] light in photonic lattices,[25,26] and light or photons in quantum-walk architectures,[27–30] or even via Bose–Einstein condensates.[31,32] However, no effect of disorder has even been observed in a non-Hermitian system.

Quantum walks provide a good testbed for quantum computations,[33] quantum communications,[34,35] quantum measurements,[36] and quantum simulations.[18,37–40] In this paper, we present the experimental realization of PT-symmetric quantum walks for single photons[41–47] with controlled dynamics, in which controllable coin operations allow us to simulate different environmental influences including static disorder and dynamic disorder.

2. Theoretical model

Firstly, we define a split-step unitary quantum walk described by the operator

$$U = SC(\theta_2)SC(\theta_1), \tag{1}$$

where $S = \sum_x |x\rangle\langle x+1| \otimes |0\rangle\langle 0| + |x\rangle\langle x-1| \otimes |1\rangle\langle 1|$ is the conditional position shift operator, and $C(\theta) = \sum_x |x\rangle\langle x| \otimes \begin{pmatrix} \cos\theta & \sin\theta \\ \sin\theta & -\cos\theta \end{pmatrix}$ is the coin operator. Here x denotes the position of a walker and $\{|0\rangle, |1\rangle\}$ are two orthogonal coin states. The unitary operator U can be extended to a non-unitary operator as

$$U_{\rm ll} = LSC(\theta_2)L'SC(\theta_1), \tag{2}$$

with the loss operators $L = \sum_x |x\rangle\langle x| \otimes \begin{pmatrix} L_1 & 0 \\ 0 & L_2 \end{pmatrix}$ and $L' = \sum_x |x\rangle\langle x| \otimes \begin{pmatrix} L_2 & 0 \\ 0 & L_1 \end{pmatrix}$, where $0 \leqslant L_1, L_2 \leqslant 1$.

For comparison, another non-unitary split-step quantum walk with gain and loss is governed by the operator

$$U_{\rm gl} = GSC(\theta_2)G^{-1}SC(\theta_1), \tag{3}$$

where $G = \sum_x |x\rangle\langle x| \otimes \begin{pmatrix} g & 0 \\ 0 & 1/g \end{pmatrix}$ denotes the gain–loss operator. This quantum walk governed by the operator $U_{\rm gl}$ has PT symmetry, i.e, $\mathcal{PT}U_{\rm gl}\mathcal{PT}^{-1}$ with $\mathcal{PT} = \sum_x |-x\rangle\langle x| \otimes \sigma_z\mathcal{K}$ ($\mathcal{K}$ is a complex conjugation operator). If we choose $g = \sqrt{L_1/L_2}$, then we have the relation

$$cU_{\rm ll} = U_{\rm gl}, \tag{4}$$

with $c = 1/(L_1L_2)$. Thus the non-unitary split-step quantum walk with loss less and loss more can be translated to the quantum walk with gain and loss which has been proven to have PT symmetry. On the other hand, by employing the above relation, we can translate results observed in the experiment of the quantum walk with only losses into those of the quantum walk with gain and loss.

For quantum walks with temporally alternating photon losses, the quasi-eigenenergy ε is defined from the eigenvalues of the time-evolution operator

$$U_{\rm ll}|\psi_\lambda\rangle = \lambda|\psi_\lambda\rangle, \quad \lambda = {\rm e}^{-{\rm i}\varepsilon+\varepsilon_0}, \tag{5}$$

[†]Corresponding author. E-mail: genp.eux@gmail.com

© 2022 Chinese Physical Society and IOP Publishing Ltd

where ε is complex, in general, and ε_0 is a negative real number. However, when $U_{\rm gl}$ $(=\mathrm{e}^{-\varepsilon_0}U_{\rm ll})$ possesses PT symmetry and the eigenstate $|\psi_\lambda\rangle$ is the eigenstate of the PT symmetry operator, ε is guaranteed to be real. Here we derive the eigenvalue of the PT-symmetric non-unitary quantum walks in the homogeneous system, and derive the condition that the quasi-eigenenergy ε becomes real.

To this end, by assuming that angles of coin operators θ_1 and θ_2 are constants over the position space, we describe the non-unitary time-evolution operator $U_{\rm gl}$ in the momentum space. With the Fourier transformation, the coin, conditional position shift, and gain–loss operators are rewritten respectively as

$$C(\theta)=\sum_k|k\rangle\langle k|\otimes\tilde{R}(\theta)\sigma_z,\quad \tilde{R}(\theta)=\mathrm{e}^{-\mathrm{i}\theta\sigma_y},\tag{6}$$

$$S=\sum_k|k\rangle\langle k|\otimes\tilde{S}(k),\quad \tilde{S}(k)=\mathrm{e}^{\mathrm{i}k\sigma_z},\tag{7}$$

$$G=\sum_k|k\rangle\langle k|\otimes\tilde{G},\quad \tilde{G}=\mathrm{e}^{\gamma\sigma_z}.\tag{8}$$

Accordingly, the time-evolution operator of non-unitary quantum walks fitted in the symmetry time flame in the momentum representation is written as

$$\begin{aligned}U'_{\rm gl}&=\sum_k|k\rangle\langle k|\otimes U'_{\rm gl}(k),\\ U'_{\rm gl}(k)&=\mathrm{e}^{\mathrm{i}\pi}\tilde{R}\Big(\frac{\theta_1}{2}\Big)\tilde{G}\tilde{S}\Big(k-\frac{\pi}{2}\Big)\tilde{R}(\theta_2)\\ &\quad\times\tilde{G}^{-1}\tilde{S}\Big(k-\frac{\pi}{2}\Big)\tilde{R}\Big(\frac{\theta_1}{2}\Big),\end{aligned}\tag{9}$$

where we use the relation $\sigma_z=\mathrm{e}^{\mathrm{i}\pi/2}\mathrm{e}^{-\mathrm{i}\pi/2\sigma_z}$. As explained in Ref. [48], we proceed with our calculation by ignoring the prefactor $\mathrm{e}^{\mathrm{i}\pi}=-1$ which only shifts the quasi-eigenenergy by π and take it into account when we need it. By also redefining $k-\pi/2$ as k, we rewrite the time-evolution operator, $\tilde{U}'_{\rm gl}(k)$, as

$$\tilde{U}'_{\rm gl}(k)=\tilde{R}\Big(\frac{\theta_1}{2}\Big)\tilde{G}\tilde{S}(k)\tilde{R}(\theta_2)\tilde{G}^{-1}\tilde{S}(k)\tilde{R}\Big(\frac{\theta_1}{2}\Big).$$

Since all the operators can be expressed by Pauli matrices, the time-evolution operator is also written as

$$\begin{aligned}&\tilde{U}'_{\rm gl}(k)=d_0(k)\sigma_0+d_x\sigma_x+\mathrm{i}d_y(k)\sigma_y+\mathrm{i}d_z(k)\sigma_z,\\ &d_0(k)=\cos\theta_1\cos\theta_2\cos(2k)-\sin\theta_1\sin\theta_2\cosh(2\gamma),\\ &d_x=-\sin\theta_2\sinh(2\gamma),\\ &d_y(k)=-\sin\theta_1\cos\theta_2\cos(2k)-\cos\theta_1\sin\theta_2\cosh(2\gamma),\\ &d_z(k)=\cos\theta_2\sin(2k).\end{aligned}\tag{10}$$

Note that, a relation $d_0^2(k)-d_x^2+d_y^2(k)+d_z^2(k)=1$ is satisfied.

The eigenvalue $\lambda_{\rm gl}$ of $\tilde{U}_{\rm gl}(k)$ is derived as follows:

$$\lambda_{\rm gl}=d_0(k)\pm\mathrm{i}\sqrt{1-d_0^2(k)}=\mathrm{e}^{-\mathrm{i}\varepsilon}.$$

Since the presence of PT symmetry guarantees $|\lambda_{\rm gl}|=1$, we find that the value of $d_0(k)$ determines that the system is in the unbroken PT-symmetric phase ($|d_0(k)|<1$ for all $k\in[0,2\pi)$), the broken PT-symmetric phase ($|d_0(k)|>1$, at least, for some k), or at the exceptional point ($|d_0(k_*)|=1$ for some k_* and $|d_0(k)|<1$ for other k).

Therefore, by recovering the prefactor of the right hand side of Eq. (9), the real and imaginary parts of the eigenvalue λ of the non-unitary quantum walks with alternating losses, $U_{\rm ll}$, is described as follows:

$$\mathrm{Re}(\lambda)=\begin{cases}-\mathrm{e}^{\varepsilon_0}d_0(k), & \text{for } |d_0(k)|\le 1,\\ -\mathrm{e}^{\varepsilon_0}\left[d_0(k)\pm\sqrt{d_0^2(k)-1}\right], & \text{for } |d_0(k)|>1,\end{cases}$$

$$\mathrm{Im}(\lambda)=\begin{cases}\pm\mathrm{e}^{\varepsilon_0}\sqrt{1-d_0^2(k)}, & \text{for } |d_0(k)|\leqslant 1,\\ 0, & \text{for } |d_0(k)|>1.\end{cases}$$

Accordingly, the real and imaginary parts of the quasi-eigenenergy ε are described as follows:

$$\mathrm{Re}(\varepsilon)=\begin{cases}\pm\arccos(-d_0(k)), & \text{for } |d_0(k)|\leqslant 1,\\ 0, & \text{for } |d_0(k)|>1,\end{cases}$$

$$\mathrm{Im}(\varepsilon)=\begin{cases}0, & \text{for } |d_0(k)|\leqslant 1,\\ \pm\mathrm{arcosh}(-d_0(k)), & \text{for } |d_0(k)|>1.\end{cases}$$

We show the presence or absence of complex quasi-eigenenergies in Fig. 1. When the PT symmetry is unbroken, all quasi-eigenenergies are all real and are plotted in the light blue squares. Whereas, when the PT symmetry is broken, quasi-eigenenergies are complex and shown in the light red areas. The size of the light red area is due to the loss parameter. Here we choose $l_1=1$ and $l_2=0.8$. The colored dots denote the parameters we choose for experiments.

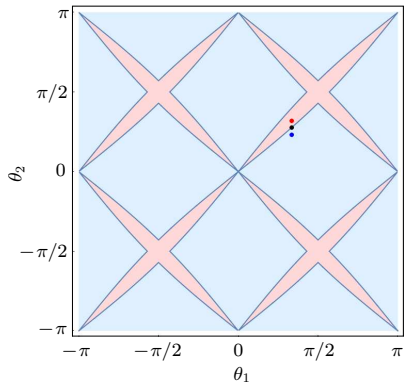


Fig. 1. Presence or absence of complex quasi-eigenenergies. When PT symmetry is unbroken, all quasi-eigenenergies are all real and are plotted in the light blue squares. Whereas, when PT symmetry is broken, quasi-eigenenergies are complex and shown in the light red areas. The size of the light red area is due to the loss parameter. Here we choose $L_1=1$ and $L_2=0.8$. The colored dots denote the parameters we choose for experiments of quantum walk in the unbroken PT-symmetric phase ($\{\theta_1=\pi/3,\theta_2=0.23\pi\}$, red dot), at the exceptional point ($\{\theta_1=\pi/3,\theta_2=0.2754\pi\}$, black dot), and in the broken PT-symmetric phase ($\{\theta_1=\pi/3,\theta_2=0.32\pi\}$, blue dot), respectively.

3. Experimental realization

In our experiment, we implement a passive PT-symmetric non-unitary split-step quantum walk with single photons,

which propagate in the cascaded interferometric network as illustrated in Fig. 2. A pair of photons is generated via the spontaneous parametric down conversion (SPDC) in the periodically poled potassium titanyl phosphate crystal (PPKTP), with one serving as a trigger and the other as a quantum walker projected into the cascaded interferometric network. The walker state $|x\rangle$ is encoded in the spatial modes of the walker photon and the coin state in the basis $\{|H\rangle, |V\rangle\}$ is encoded in the polarizations of the walker photon. The initial state of the walker+coin system is prepared in $|0\rangle(|H\rangle + \mathrm{i}|V\rangle)/\sqrt{2}$ via a polarizing beam splitter (PBS), a half-wave plate (HWP), and a quarter-wave plate (QWP). The coin operation $C(\theta)$ is implemented by a HWP at the setting angle $\theta/2$. Whereas, the shift operator S is implemented via a birefringent beam displacer (BD) through which horizontally polarized photons are directly transmitted and vertically polarized photons undergo a lateral displacement into a neighboring mode. The loss operator L is implemented via a partially polarizing beam splitter (PPBS) with the transmissivity of horizontally and vertically polarized photons $(T_H, T_V) = (L_1^2, L_2^2)$, while L' is implemented via a sandwich-type setup (HWP-PPBS-HWP). As we realize a passive PT-symmetric quantum walk, for the probability distribution, we need the corrected probability instead of the normalized probability $P_{\mathrm{N}}(x,t)$ which is obtained directly via a coincidence measurement. The corrected probability $P_{\mathrm{C}}(x,t) = c^{2t}\sum_{x'} P_{\mathrm{th}}(x',t)P_{\mathrm{N}}(x,t)$ is obtained by multiplying both the theoretical prediction of the sum of the probabilities P_{th} and the correction factor $c = 1/(L_1L_2)$ for the respective step t.

Two types of disorders, static disorder and dynamic disorder, are considered in our experiment. The static disorder is introduced to the coin rotations by modulating the angles of the corresponding HWPs by a small random amount $\delta\theta$ around the coin parameters $\theta_{1,2}$. Here $\delta\theta \in \left[-\frac{\pi}{26}, \frac{\pi}{26}\right]$ is position-independent but unique for each time-step. We then implement quantum-walk dynamics governed by the evolution operator U_{ll} with randomly generated coin rotations $C(\theta_{1,2} + \delta\theta)$ instead of $C(\theta_{1,2})$.

On the other hand, we can also introduce dynamic disorder to the coin rotation. To introduce dynamic disorder, a time-dependent coin rotation with randomly generated coin parameters $\theta_{1,2} + \delta\theta$ is required. In our experiment, the setting angles of HWPs for each step are modulated by a small random amount $\delta\theta$ around the coin parameters (θ_1, θ_2). The strength of the disorder is determined by the shift $\delta\theta$. In order to compare the influences of static disorder and dynamic disorder, we keep the same interval $\delta\theta \in \left[-\frac{\pi}{26}, \frac{\pi}{26}\right]$ for both cases. Note that $\delta\theta$ here is time-dependent but unique for each position. We then push the time-step of the PT-symmetric quantum-walk dynamics with either static disorder or dynamic disorder up to 6 and compare the behavior of the quantum walker under the different environmental influences.

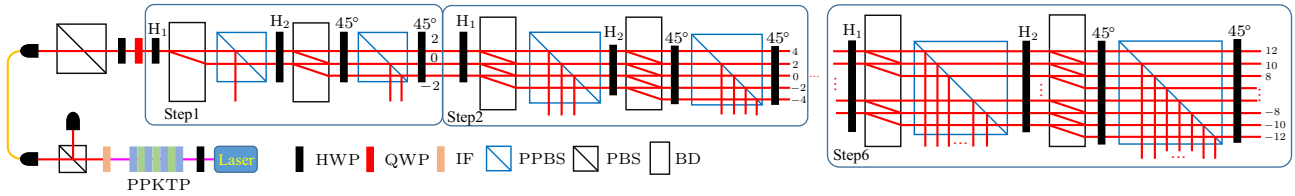


Fig. 2. Experimental setup. Photons in pair are generated via the SPDC in PPKTP, with one serving as a trigger photon and the other as the quantum walker projected into the quantum-walk network. The coin operation C is implemented by a HWP and the shift operator S is implemented via a BD. The loss operator L is implemented via a PPBS. Photons appearing in the spatial modes at the output of the quantum-walk network are detected by single photon detectors (as known as APDs), in coincidence with the trigger photon.

4. Experimental results

We experimentally analyse the PT-symmetric quantum walk with various coin angles $(\theta_1, \theta_2) = (\pi/3, 0.23\pi)$, $(\theta_1, \theta_2) = (\pi/3, 0.2754\pi)$, and $(\theta_1, \theta_2) = (\pi/3, 0.32\pi)$, respectively, and with fixed loss parameters $(L_1, L_2) = (1, 0.8)$ as illustrated in Fig. 1. For the fist case with the choice of the coin parameters $(\theta_1, \theta_2) = (\pi/3, 0.23\pi)$, the quasi-eigenenergies of the walker+coin system remain entirely real and the corresponding non-unitary time evolution preserves PT symmetry. For the second case of the choice of the coin parameters $(\theta_1, \theta_2) = (\pi/3, 0.2754\pi)$, the PT-symmetric quantum walk is now at the exceptional point from the unbroken to broken PT-symmetric phase. For the third case, by further increasing the coin parameter θ_2 to 0.32π and keeping θ_1 unchanged, the walker+coin system enters the broken PT-symmetric phase, in which the quasi-eigenenergies of the system are typically complex. The corrected probability distribution of the PT-symmetric quantum walk up to 6 steps and the variance of the distribution are shown in Fig. 3. We can see that the experimental results represented by symbols agree well with those obtained by numerical simulations represented by curves. We can also see that for the PT unbroken case, the corrected probability distribution is almost the same as that of the standard unitary quantum walk.

For the second case, at the exceptional point, the corrected probability distribution is different from that of the standard unitary quantum walk as the peaks are squeezed a bit. However, by comparing the variances of the distributions for the two cases, we confirm that even at the exception point, the behavior of the walker is still ballistic.

However, for the PT broken case, the corrected probability distribution and the variance become completely different

from the standard unitary quantum walk. The distribution is now Gaussian-like, which is a typical phenomenon in the broken PT-symmetric phase. The variance also confirms that the walk shows a diffusive behavior.

In Figs. 4–6, considering both static and dynamic disorders, the coin rotations take the angles $\theta_{1,2}+\delta\theta$, where $\delta\theta$ is randomly chosen from the interval $\left[-\frac{\pi}{26},\frac{\pi}{26}\right]$, and is position-dependent for static disorder and time-dependent for dynamic disorder, respectively. Compared to the PT-symmetric quantum walk without any disorder, the influence of dynamic disorder reduces the expansion of the wavefunction to the level of a diffusive classical particle for all the cases of PT unbroken, PT broken, and exception point. That is, for all the three cases, the behavior of the quantum walker turns to be diffusive, as a classical particle.

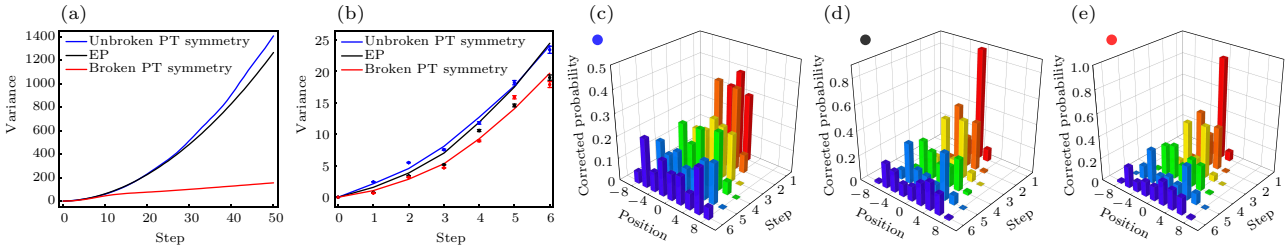


Fig. 3. Experimental results of the PT-symmetric quantum walk with the coin angles $(\theta_1,\theta_2)=(\pi/3,0.23\pi)$, $(\theta_1,\theta_2)=(\pi/3,0.2754\pi)$, and $(\theta_1,\theta_2)=(\pi/3,0.32\pi)$, respectively, and with loss parameters $(L_1,L_2)=(1,0.8)$. Variances for the quantum walk up to 50 in (a) and 6 steps in (b) vs. the number of the steps. Colored curves indicate the numerical simulations of the variances, while experimental results are presented by symbols. Experimental errors are due to photon counting statistics. (c)–(e) Experimental results of the probability distributions for all the three cases of PT unbroken, PT broken, and exception point, respectively.

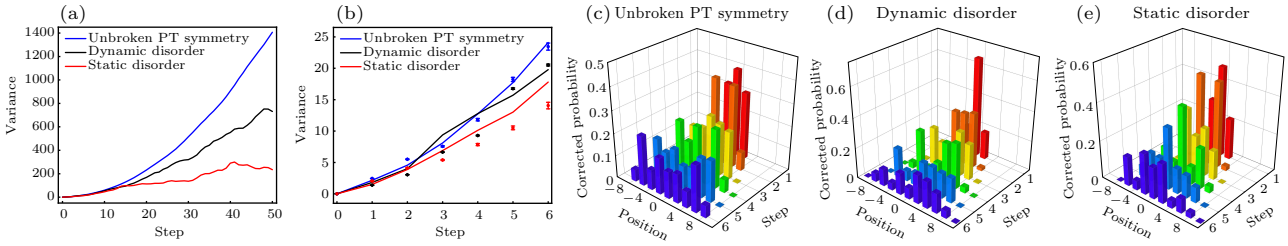


Fig. 4. Experimental results of the disordered PT-symmetric quantum walk with the coin angles $(\theta_1,\theta_2)=(\pi/3,0.23\pi)$ and with loss parameters $(L_1,L_2)=(1,0.8)$. The walker+coin system is in the PT unbroken phase. Variances for the quantum walk up to 50 in (a) and 6 steps in (b) vs. the number of the steps. Colored curves indicate the numerical simulations of the variances, while experimental results are presented by symbols. Experimental errors are due to photon counting statistics. (c)–(e) Experimental results of the probability distributions of the PT-symmetric quantum walk in the PT unbroken phase without disorder, with dynamic disorder, and with static disorder, respectively.

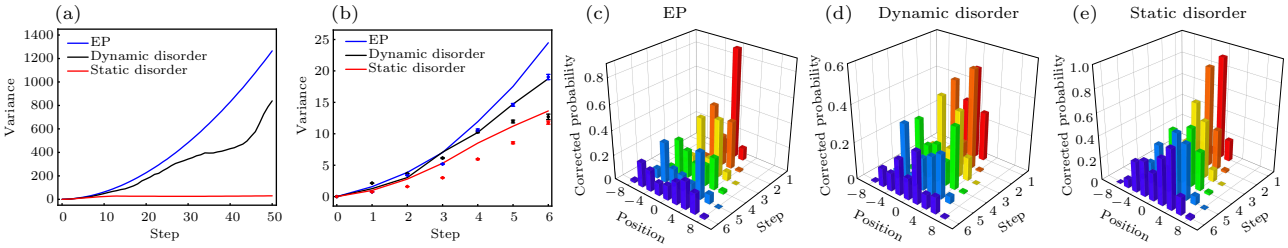


Fig. 5. Experimental results of the disordered PT-symmetric quantum walk with the coin angles $(\theta_1,\theta_2)=(\pi/3,0.2754\pi)$ and with loss parameters $(L_1,L_2)=(1,0.8)$. The walker+coin system is at the exceptional point. Variances for the quantum walk up to 50 in (a) and 6 steps in (b) vs. the number of the steps. Colored curves indicate the numerical simulations of the variances, while experimental results are presented by symbols. Experimental errors are due to photon counting statistics. (c)–(e) Experimental results of the probability distributions of the PT-symmetric quantum walk at the exception point without disorder, with dynamic disorder, and with static disorder, respectively.

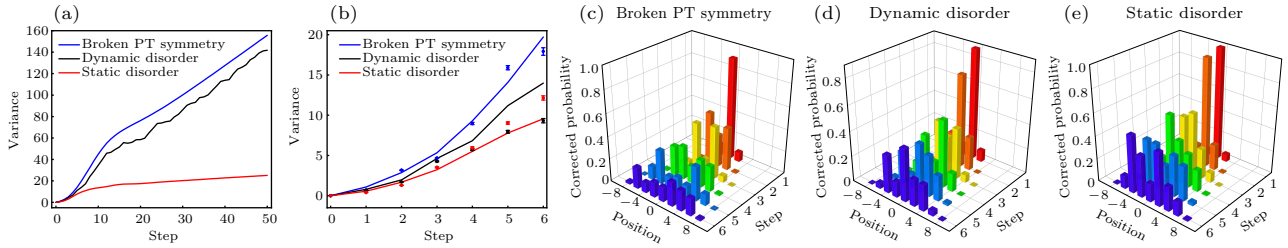


Fig. 6. Experimental results of the disordered PT-symmetric quantum walk with the coin angles $(\theta_1,\theta_2)=(\pi/3,0.32\pi)$ and with loss parameters $(L_1,L_2)=(1,0.8)$. The walker+coin system is in the PT broken phase. (a), (b) Variances vs. the number of the steps. Colored curves indicate the numerical simulations of the variances and the experimental results are presented by symbols. Experimental errors are due to photon counting statistics. (c)–(e) Experimental results of the probability distributions of the PT-symmetric quantum walk in the PT broken phase without disorder, with dynamic disorder, and with static disorder, respectively.

On the other hand, the influence of static disorder stops the spread of the walker and leads to a localization for all the three cases. The localization is further confirmed by smaller variances for all the three cases. Our experimental investigations show how the two kinds of disorders influence the behavior of the quantum walker in the PT-symmetric quantum dynamics.

5. Conclusion

We experimentally investigate how dynamic disorder and static disorder can influence the non-unitary evolution of a PT-symmetric quantum walk and show the controlled transition between the different regimes. We realize a passive PT-symmetric quantum dynamics of single photons via temporally alternating photon losses in the cascaded interferometric network. Furthermore, via controllable coin operations we simulate different environmental influences of both dynamic and static disorders on the walker+coin system, which result in a standard ballistic spread, a classical diffusive behavior, and a localization of the walker in a PT-symmetric quantum walk architecture, respectively. Our setup of the single-photon implementation of PT-symmetric quantum walks with high flexibility and full control allows us not only to study the interesting features in non-Hermitian quantum dynamics but also to simulate interesting scenarios for the community of condensed matter physics and high-energy physics. Our experimental results suggest exciting methods for the investigation of Anderson localization of non-Hermitian systems using one-dimensional discrete-time quantum walks.

Acknowledgment

This work was supported by the National Natural Science Foundation of China (Grant Nos. 12025401 and U1930402).

References

[1] Bender C M and Boettcher S 1998 *Phys. Rev. Lett.* **80** 5243
[2] Bender C M, Berntson B K, Parker D and Samuel E 2013 *Am. J. Phys.* **81** 173
[3] Rüter C E, Makris K G, El-Ganainy R, Demetrios N, Christodoulides D N, Segev M and Detlef Kip D 2010 *Nat. Phys.* **6** 192
[4] Regensburger A, Bersch C, Miri M A, Onishchukov G, Christodoulides D N and Peschel U 2012 *Nature* **488** 167
[5] Lee S B, Yang J, Moon S, Lee S Y, Shim J B, Kim S W, Lee J H and An K 2009 *Phys. Rev. Lett.* **103** 134101
[6] Dembowski C, Gräf H D, Harney H L, Heine A, Heiss W D, Rehfeld H and Richter A 2001 *Phys. Rev. Lett.* **86** 787
[7] Brandstetter M, Liertzer M, Deutsch C, Klang P, Schöberl J, Türeci H E, Strasser G, Unterrainer K and Rotter S 2014 *Nat. Commun.* **5** 4034
[8] Xu H, Mason D, Jiang L and Harris J G E 2016 *Nature* **537** 80
[9] Guo A, Salamo G J, Duchesne D, *et al.* 2009 *Phys. Rev. Lett.* **103** 093902
[10] Xiao L, Zhan X, Bian Z H, *et al.* 2017 *Nat. Phys.* **13** 1117
[11] Li J, Harter A K, Liu J, Melo L de, Joglekar Y N and Luo L 2019 *Nat. Commun.* **10** 855
[12] Peng B, Özdemir Ş K, Lei F, Monifi F, Gianfreda M, Long G L, Fan S, Nori F, Bender C M and Yang L 2014 *Nat. Phys.* **10** 394
[13] Chang L, Jiang X, Hua S, Yang C, Wen J, Jiang L, Li G, Wang G and Xiao M 2014 *Nat. Photon.* **8** 524
[14] Feng L, Wong Z J, Ma R M, Wang Y and Zhang X 2014 *Science* **346** 972
[15] Zhan X, Xiao L, Bian Z H, Wang K K, Qiu X Z, Sanders B C, Yi W and Xue P 2017 *Phys. Rev. Lett.* **119** 130501
[16] Xiao L, Wang K K, Zhan X, Bian Z H, Kawabata K, Ueda M, Yi W and Xue P 2019 *Phys. Rev. Lett.* **123** 230401
[17] Wang K K, Qiu X Z, Xiao L, Zhan X, Bian Z H, Yi W and Xue P 2019 *Phys. Rev. Lett.* **122** 020501
[18] Li T Y, Zhang Y S and Yi W 2021 *Chin. Phys. Lett.* **38** 030301
[19] Xiao L, Deng T S, Wang K K, Zhu G Y, Wang Z, Yi W and Xue P 2020 *Nat. Phys.* **16** 761
[20] Xiao L, Deng T S, Wang K K, Wang Z, Yi W and Xue P 2021 *Phys. Rev. Lett.* **126** 230402
[21] Wang K K, Xiao L, Budich J C, Yi W and Xue P 2021 *Phys. Rev. Lett.* **127** 026404
[22] Xia S, Kaltsas D, Song D, Komis I, Xu J, Szameit A, Buljan H, Makris K G and Chen Z 2021 *Science* **3** 72
[23] Anderson P W 1958 *Phys. Rev.* **109** 1492
[24] Wiersma D S, Bartolini P, Lagendijk A and Righini R 1997 *Nature* **390** 671
[25] Lahini Y, Avidan A, Pozzi F, Sorel M, Morandotti R, Christodoulides D N and Silberberg Y 2008 *Phys. Rev. Lett.* **100** 013906
[26] Schwartz T, Bartal G, Fishman S and Segev M 2007 *Nature* **446** 52
[27] Schreiber A, Cassemiro K N, Potoček V, Gábris A, Jex I and Silberhorn C 2011 *Phys. Rev. Lett.* **106** 180403
[28] Crespi A, Osellame R, Ramponi R, Giovannetti V, Fazio R, Sansoni L, De Nicola F, Sciarrino F and Mataloni P 2013 *Nat. Photon.* **7** 322
[29] Xue P, Qin H and Tang B 2014 *Scientific Reports* **4** 04825
[30] Xue P, Zhang R, Bian Z, Zhan X, Qin H and Sanders B C 2015 *Phys. Rev. A* **92** 042316
[31] Roati G, D'Errico C, Fallani L, Fattori M, Fort C, Zaccanti M, Modugno G, Modugno M and Inguscio M 2008 *Nature* **453** 895
[32] Billy J, Josse V, Zuo Z, Bernard A, Hambrecht B, Lugan P, Clément D, Sanchez-Palencia L, Bouyer P and Aspect A 2008 *Nature* **453** 891
[33] Xue P and Xiao Y 2006 *Phys. Rev. Lett.* **97** 140501
[34] Xue P, Li C F and Guo G C 2001 *Phys. Rev. A* **64** 032305
[35] Xue P, Li C F and Guo G C 2002 *Phys. Rev. A* **65** 022317
[36] Bian Z H, Li J, Zhan X, Zhang R, Sanders B C and Xue P 2015 *Phys. Rev. Lett.* **114** 203602
[37] Xue P and Sanders B C 2012 *Phys. Rev. A* **85** 022307
[38] Xue P, Qin H, Tang B and Sanders B C 2014 *New J. Phys.* **16** 053009
[39] Xue P, Sanders B C, Blais A and Lalumiere K 2008 *Phys. Rev. A* **78** 042334
[40] Wang K K, Qiu X, Xiao L, Zhan X, Sanders B C, Yi W and Xue P 2019 *Nat. Commun.* **10** 2293
[41] Xue P, Sanders B C and Leibfried D 2009 *Phys. Rev. Lett.* **103** 183602
[42] Qin H and Xue P 2013 *Chin. Phys. B* **23** 010301
[43] Zhang R, Qin H, Tang B and Xue P 2013 *Chin. Phys. B* **22** 110312
[44] Xue P, Qin H, Tang B, Zhan X, Bian Z H and Li J 2014 *Chin. Phys. B* **23** 110307
[45] Xue P, Zhang R, Qin H, Zhan X, Bian Z H, Li J and Sanders B C 2015 *Phys. Rev. Lett.* **114** 140502
[46] Qin H and Xue P 2016 *Chin. Phys. B* **25** 010501
[47] Lin Q, Qin H, Wang K K, Xiao L and Xue P 2020 *Chin. Phys. B* **29** 110303
[48] Obuse H, Asbóth J K, Nishimura Y and Kawakami N 2015 *Phys. Rev. B* **92** 045424